LETTER
Published in ***Physics of Fluids***, 36, 031708 (2024). DOI: 10.1063/5.0200164

Experimental verification of rotating detonation engine with film cooling

Jingtian Yu[1,2], Songbai Yao[1,2,*], Jingzhe Li[1,3], Jianghong Li[1,3], Rujia Wang[1], Bin Wang[1,2], Wenwu Zhang[1,2]

[1]Ningbo Institute of Materials Technology and Engineering, Chinese Academy of Sciences, Ningbo 315201, China

[2]University of Chinese Academy of Sciences, Beijing 100049, China

[3]Faculty of Mechanical Engineering and Mechanics, Ningbo University, Ningbo 315211, China

[*]**Corresponding author**: yaosongbai@nimte.ac.cn (S. Yao)

Abstract

In this short letter, we report an experimental investigation on the integration of film cooling for thermal protection in a 72-mm cylindrical rotating detonation engine (RDE). The cooling scheme involves injection of cooling air through a series of cat-ear-shaped film cooling holes densely distributed along the outer wall of the cylindrical combustor. Our findings reveal the successful initiation of the RDE and sustained propagation of the rotating detonation wave (RDW) when film cooling is activated and the outflow reaches a supersonic state. Experimental observations corroborate the numerical simulations, indicating a lateral expansion tendency of the cooling jet under the influence of the high-frequency RDW.

The rotating detonation engine (RDE) is a revolutionary technology that has gained global attention in the field of aerospace propulsion due to the characteristics of pressure gain combustion (PGC), fast heat release, and higher thermodynamic cycle efficiency compared with that of traditional deflagration-based power systems [1, 2]. These unique features make it highly promising for a wide range of applications in the field of aerospace propulsion, such as the recent experimental studies [3-8]. However, detonation is an extreme combustion phenomenon. These high-frequency thermal loads [9, 10] can lead to severe wall thermal ablation within the combustion chamber. Therefore, the implementation of effective thermal protection measures is of paramount importance for advancing the engineering application of RDEs. There have been several recent attempts in this regard. Goto et al. [11] employed an injection scheme in which propellant was introduced through 24 pairs of injectors on the sidewall for temperature cooling. Tian et al. [12] revealed the interaction between the cooling air from cylindrical film holes in the rotating detonation flow field through numerical simulation and showed that the cooling air did not exert a significant influence on the propagation of the rotating detonation wave (RDW), but the RDW would periodically block the normal outflow of the cooling air. In the numerical investigation conducted by Yu et al. [13], the cooling efficiency of cylindrical film holes was evaluated under various mass flow rates of the primary flow (hydrogen and propellant air) and secondary flow (cooling air). The results revealed that as the mass flow rate of the cooling air increased, there was a significant expansion in the area of the outer wall covered by cooling air in the axial direction. Li et al. [14] numerically analyzed the cooling performance of five different cylindrical film holes with different aspect ratios arranged on the inner and outer walls of the RDE with a Laval nozzle, and determined a scheme of film hole configuration, injection parameters and nozzle configuration that considered cooling and aerodynamic performance simultaneously. In the recent work of Li et al. [15], the two-phase RDW flow field with film cooling was also investigated. As an efficient cooling method widely employed in turbine blades, film cooling offers notable advantages in terms of its flexibility and compatibility. To date, however, there is a scarcity of experimental verification regarding the feasibility of integrating film cooling for the RDE. In this study, therefore, we conduct experiments to verify the ignition and operation of a cylindrical RDE equipped with complex-shaped holes for film cooling.

The cylindrical rotating detonation combustor (RDC) has an outer diameter of $d = 72$ mm and a length of $L = 87.5$ mm, as shown in Fig. 1. In the context of film cooling, the cylindrical configuration [15-18] offers an additional advantage. This is because there is no inner cylinder necessitating thermal protection, and the fabrication of film cooling holes is only necessary on the outer wall. The RDC is equipped with a Laval nozzle with an exit-to-throat area ratio of 9. Hydrogen and air are injected at an ambient temperature using a commonly utilized orifice-slot design. The injection section consists of 200 orifices with a diameter of 0.5 mm for hydrogen injection, along with an air slot measuring 0.6 mm in width. The outer wall (thickness $\delta = 1.5$ mm) surface is machined by femtosecond laser technology to incorporate film cooling holes, each configured in a cat-ear shape. This particular design, proven to significantly enhance film cooling effectiveness, has

undergone comprehensive optimization and analysis [19]. The cat-ear-shaped configuration can lead to a larger protected area and improved adherence of cooling jets to the protected wall by the development of anti-counter-rotating vortices [20]. The shaped film holes are inclined at a 30° angle relative to the axial direction of the RDC. There are in total 13 circumferential rows of film cooling holes spaced 5-mm apart vertically, with each row consisting of 30 film cooling holes. This configuration results in a total of 390 film holes densely distributed over the outer wall, which is made of 304 stainless steel. The geometry and schematic of the cat-ear-shaped film hole can be referenced in our previous study [21].

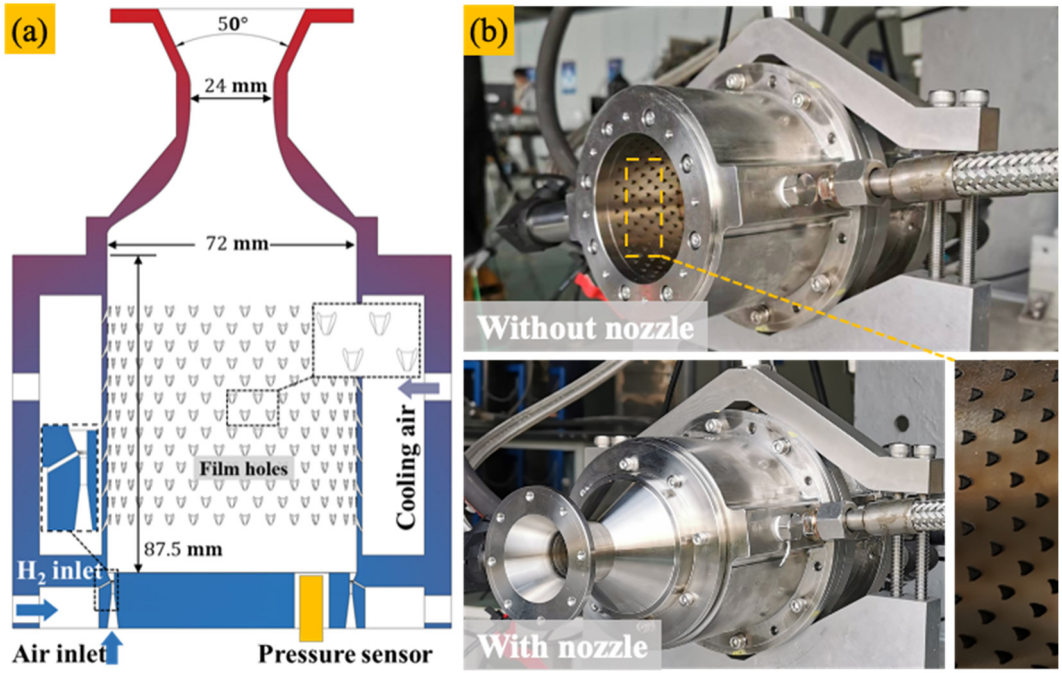

Figure 1: Cylindrical RDE with cat-ear-shaped film cooling holes: (a) front view and (b) device.

The hydrogen-fueled RDE is ignited using an automotive spark plug. Preceding the RDE ignition, cooling air is injected for a duration of 1 s at a constant mass flow rate of approximately 100 g/s and is held constant after ignition. Post-ignition, the RDE operates for 0.5 s in Shot No. 1. The high-frequency piezoresistive pressure transducer is located adjacent to the outer wall on the headwall side (see Fig. 1) for the acquisition of pressure signals of the RDW. In Shot No. 2, the duration of RDE operation is extended to 2 s, and the mass flow rate of cooling air is increased to 120 g/s, but the pressure transducers are temporarily removed to prevent high-temperature damage. The working conditions of the test shots are summarized in Table 1.

Table 1 Working conditions (mass flow rates) of the test shots.

	Hydrogen (g/s)	Air (propellant) (g/s)	Air (cooling) (g/s)
Shot 1	8.7	300	100
Shot 2	8.7	300	120

The pressure signals during the operation of Shot No. 1 are shown in Fig. 2, representing

segments of the detonation operation at a stable stage. Local views of the pressure traces at different stages are magnified to demonstrate the continued operation of the RDE. The periodic peak amplitudes caused by the detonation wave are below 0.5 MPa in the initial phase. During subsequent propagation, the peak pressures of the RDW increase to approximately 1.0 MPa. Then the pressure signals undergo high-pass filtering and are processed through a fast Fourier transform (FFT) analysis and a short-time Fourier transform (STFT) analysis. The FFT result indicates a domain frequency of approximately 10 kHz, and this is corroborated by the STFT results, showing that the domain frequency remains constant over time after the establishment of the RDW. Inferred from the domain frequency and confirmed by the phase angle of the pressure signal from another sensor installed 90° apart in the azimuthal direction, calculations suggest a detonation wave speed of 2271 m/s in a single-wave combustion mode. This is very close to the value of 2194.6 m/s reported in the experimental study by Zhang et al. [22], who also noted that a difference could exist in the behavior of the RDW between annular and cylindrical configurations, wherein the detonation wave demonstrated the potential to be overdriven in the latter.

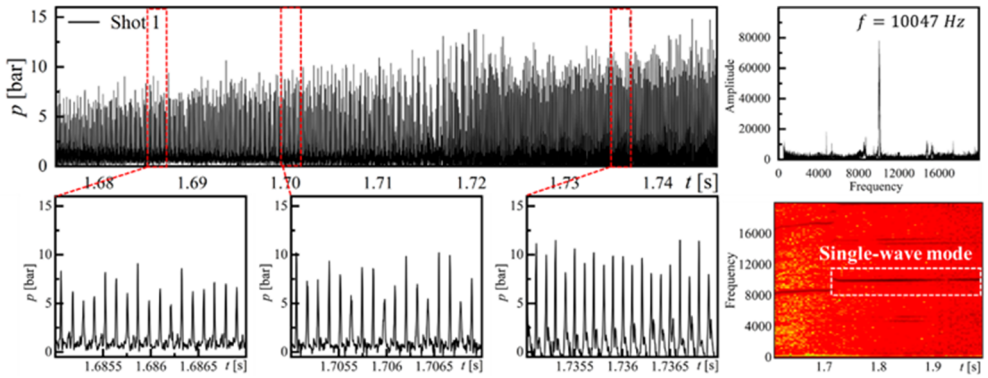

Figure 2: Pressure trace records and FFT analysis of Shot No. 1.

For Shot No. 2, which runs for 2 s, the corresponding time sequence and variations of the static pressures in the combustor and cooling air manifold are presented (Fig. 3). After ignition, the static pressure of the combustor remains almost constant at approximately 0.5 MPa, while that of the cooling air manifold slightly increases until cutoff. Figure 4 presents a comparative analysis of exhaust plume photographs from the two respective shots. Aside from variations in daylight exposures, the presence of Mach diamonds within both exhaust plumes indicates the occurrence of supersonic jets in both operational conditions.

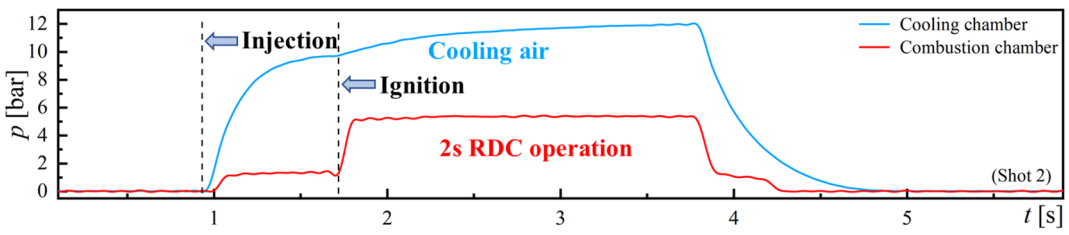

Figure 3: Time sequence and static pressure measurements in Shot No. 2.

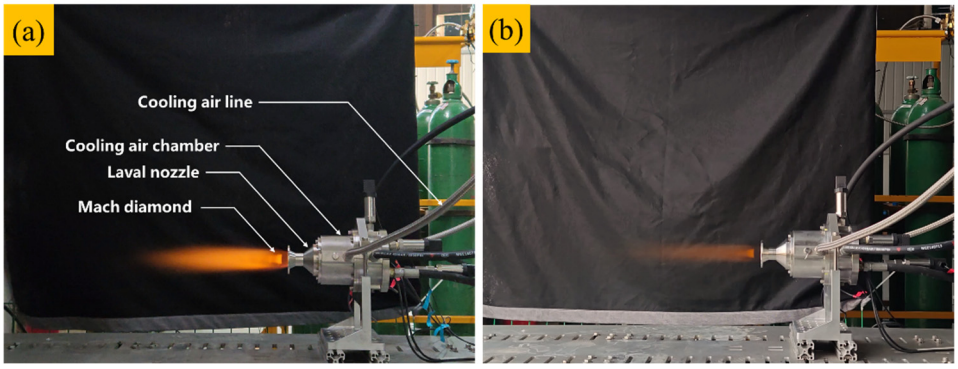

Figure 4: Exhaust plumes: (a) Shot No. 1 and (b) Shot No. 2.

Finally, the inner surface of the outer wall after Shot No. 2 is shown in Fig. 5(a). The trace of cooling air can be clearly reflected by the temperature difference of burn marks (see the zoomed region); near the film cooling holes, the wall surface is better protected by the cooling air. Additionally, the cooling jet is found to swing laterally under the influence of the RDW. These experimental findings align well with our previous numerical result [21] shown in Fig. 5(b). As the RDW passes through the film hole, the cooling jet will swing toward the propagation direction of the RDW. Since the velocity of detonation wave is several times faster than that of the cooling air, the interruptions caused by the cooling jet are not significant, and thus will not cause considerable velocity deficit of the RDW.

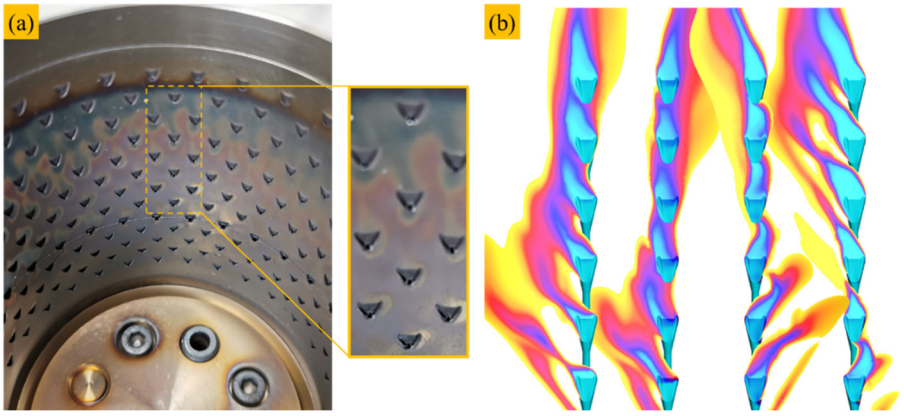

Figure 5: Film cooling air patterns within the rotating detonation flow field: (a) outer wall surface condition after operation, and (b) simulation result from Yu et al. [21].

In conclusion, our experimental investigation into the integration of film cooling for thermal protection in a cylindrical RDE has yielded some promising results. Successful initiation and sustained propagation of the RDE during the activation of film cooling are reported for both short and longer test shots. With cooling jets entering from cat-ear-shaped film holes over the outer wall, the RDE is found to operate stably, and the exhaust outflow reaches a supersonic state. The experimental findings also validate the characteristics of the cooling jet in the RDW flow field revealed by numerical simulations. Future work is required to conduct a more comprehensive investigation to evaluate the film cooling performance.

References

[1] J.Z. Ma, M.Y. Luan, Z.J. Xia, J.P. Wang, S.J. Zhang, S.B. Yao, B. Wang, AIAA Journal, 58 (2020) 4976-5035.

[2] V. Raman, S. Prakash, M. Gamba, Annual Review of Fluid Mechanics, 55 (2023) 639-674.

[3] S. Gray, M. McLoughlin, G. Ciccarelli, Combustion and Flame, 260 (2024).

[4] S. Zhou, Y. Ma, F. Liu, N. Hu, Fuel, 354 (2023).

[5] X. Yang, Y. Wu, F. Song, J. Zhou, H. Liu, S. Xu, X. Chen, Experimental Thermal and Fluid Science, 146 (2023).

[6] Y. Wu, G. Xu, C. Ding, C. Weng, Physics of Fluids, 35 (2023) 016128.

[7] C. Knowlen, T. Mundt, M. Kurosaka, Shock Waves, (2023).

[8] M. Kawalec, P. Wolański, W. Perkowski, A. Bilar, Journal of Propulsion and Power, (2023) 1-8.

[9] Y. Qiu, Y. Wu, Y. Huang, Q. Li, C. Weng, Physics of Fluids, 36 (2024) 016131.

[10] D. Lim, S.D. Heister, J. Humble, A.J. Harroun, Journal of Spacecraft and Rockets, 58 (2021) 1444-1452.

[11] K. Goto, K. Ota, A. Kawasaki, N. Itouyama, H. Watanabe, K. Matsuoka, J. Kasahara, A. Matsuo, I. Funaki, H. Kawashima, Journal of Propulsion and Power, 38 (2022) 410-420.

[12] J. Tian, Y.-s. Wang, J.-z. Zhang, X.-m. Tan, Aerospace Science and Technology, 122 (2022).

[13] J. Yu, S. Yao, J. Li, Y. Huang, C. Guo, W. Zhang, International Journal of Hydrogen Energy, 48 (2023) 9082-9094.

[14] R. Li, J. Xu, H. Lv, D. Lv, J. Song, Aerospace Science and Technology, 136 (2023) 108221.

[15] J. Li, J. Yu, J. Li, Y. Lei, S. Yao, W. Zhang, Physics of Fluids, 36 (2024).

[16] R. Wiggins, A. Gaetano, T. Pritschau, J. Betancourt, V. Shaw, V. Anand, E. Gutmark, AIAA Journal, (2022) 1-11.

[17] S.-Y. Huang, J. Zhou, S.-J. Liu, H.-Y. Peng, X.-Q. Yuan, H.-L. Zhang, Combustion and Flame, 248 (2023).

[18] G. Rong, M. Cheng, Z. Sheng, X. Liu, Y. Zhang, J. Wang, Physics of Fluids, 34 (2022) 056104.

[19] K. Kusterer, N. Tekin, D. Bohn, T. Sugimoto, R. Tanaka, M. Kazari, in: ASME Turbo Expo 2012: Turbine Technical Conference and Exposition, 2012, pp. 1299-1310.

[20] K. Kusterer, A. Elyas, D. Bohn, T. Sugimoto, R. Tanaka, M. Kazari, in: ASME 2011 Turbo Expo: Turbine Technical Conference and Exposition, 2011, pp. 303-313.

[21] J. Yu, S. Yao, J. Li, J. Li, C. Guo, W. Zhang, Aerospace Science and Technology, (2023) 108642.

[22] H. Zhang, W. Liu, S. Liu, International Journal of Hydrogen Energy, 41 (2016) 13281-13293.